Supplement of

Reconstructed glacier area and volume changes in the European Alps since the Little Ice Age

Johannes Reinthaler[1], Frank Paul[1]

[1] Department of Geography, University of Zurich, Zurich, Switzerland

Correspondence: Johannes Reinthaler (johannes.reinthaler@geo.uzh.ch)

Content:

1 Supplementary tables

Table S1: List of historical maps with glacier extents available for the different Alpine countries.

County	Name	Date	Scale	Link
Switzerland	Dufour map	1845-1865	1:100000	https://www.swisstopo.admin.ch/en/geodata/maps/historical/dufour.html
	Siegfried map	1870-1926	1:50000	https://www.swisstopo.admin.ch/en/geodata/maps/historical/siegfried25.html
France	Carte de l'état major	1820-1866	1:40000	https://www.geoportail.gouv.fr/donnees/carte-de-letat-major-1820-1866
Italy	Übersichtskarte der Dolomiten	1903	1:100000	https://www.e-rara.ch/zut/content/titleinfo/29139322
	Austro-Hungarian Monarchy. Militärgeographisches Institut, Zone 19 col 6 (Toblach & Cortina d' Ampezzo)	1889	1:75000	https://digitalcollections.nypl.org/items/510d47df-8b8d-a3d9-e040-e00a18064a99
	Austro-Hungarian Monarchy. Militärgeographisches Institut, Zone 20 col 5 (Bozen & Fleimstal)	1882	1:75000	https://digitalcollections.nypl.org/items/510d47df-8bae-a3d9-e040-e00a18064a99
	Austro-Hungarian Monarchy. Militärgeographisches Institut, Zone 20 col 6 (Pieve Di Livinallongo und Longarone)	1882	1:75000	https://digitalcollections.nypl.org/items/510d47df-8bb0-a3d9-e040-e00a18064a99
Germany	Topographische Karte von Bayern 869, Hochkarlter 888, Zugspitze 870/871, St Bartholomä	1889-1897	1:25000	https://www.geodaten.bayern.de/histTopoKarten/01_Positionsblatt/01_869_F_1923.pdf https://www.geodaten.bayern.de/histTopoKarten/01_Positionsblatt/01_888_F_1936.pdf https://www.geodaten.bayern.de/histTopoKarten/01_Positionsblatt/01_870_F_1937.pdf
Slovenia	Studi Alpini fatti nella valle della Raccolana - Giacomo Savorgnan di Brazzà	1881	1:32000	https://www.abebooks.it/STUDI-ALPINI-FATTI-VALLE-RACCOLANA-Alpi/22916664602/bd

Table S2: Existing glacier outlines used for this study and their sources.

Country	Name, Reference	Date	Nr. glaciers	Mapping approach	Data Access
All	RGI 7, (Pfeffer et al., 2014; RGI 7.0 Consortium, 2023)	2003	4034	Satellite image mapping	Open access
Switzerland	(Paul et al., 2020)	2015	4395	Sentinel-2	Open access
	(Maisch et al., 2000)	LIA	2380	Digitisation of Siegfried map	GLIMS
	(Müller et al., 1976)	1973	2061	Areal photographs	glamos.ch
Austria	(Fischer et al., 2015)	LIA	645	Update of existing inventory using lidar and orthophotos	GLIMS
France	(Groß, 1987)	1969	869		GLIMS
	(Gardent and Deline, 2011)	LIA	269	Digitisation using maps, photographs and field investigation	Open access dataset
	(Vivian, 1975)	1967-71	502		GLIMS
Italy (Aosta)	GlaRiskAlp	LIA	210		Open access dataset
Italy (Piemonte)	(Lucchesi et al., 2014)	LIA	96		Open access dataset
Italy (Trentino)	(Zanoner et al., 2017)	LIA	159	Mapping using Lidar and high res. orthophotos	Dataset shared by the author
Italy (South Tyrol)	(Knoll et al., 2009)	LIA	300	Digitisation using high res. DEM, orthophotos and historic maps	Dataset shared by the author
Italy (Friuli) and Slovenia	(Colucci and Žebre, 2016)	LIA	20		Dataset shared by the author

Table S3: Previously missing glaciers and glaciers with new LIA outlines.

Region ID	Region name	Nr. of previously missing glacier (rgi v7.0)	Area (rgi v7.0) km^2	Glacier count (rgi v7) with new LIA outlines	Area (rgi v7.0) with new LIA outlines	Glacier count with no LIA outline	Area (rgi v7.0) with no LIA outlines
1	Dauphiné Alps	294	71.19	163	66.99	131	4.21
2	Cottian & Maritime Alps	10	0.30	1	0.06	9	0.23
3	Graian Alps	30	1.33	1	0.23	29	1.10
4	Savoy Prealps	18	3.17	11	2.95	7	0.23
5	Pennine Alps	32	13.54	17	12.83	15	0.70
6	Bernese Alps	19	3.38	1	2.84	18	0.54
7	Glarus Alps	4	0.14			4	0.14
8	Lepontine Alps	43	7.31	19	6.70	24	0.61
9	Rhaetian Alps West	179	39.47	81	36.50	98	2.97
10	Rhaetian Alps East	2	0.03			2	0.03
11	Rhaetian Alps South	74	41.05	58	40.49	16	0.56
12	Tauern Alps West	18	2.32	7	2.03	11	0.29
13	Dolomites & Carnic Alps	33	2.33	22	1.94	11	0.39
14	Northeastern Alps	11	0.91	8	0.81	3	0.10
Total		767	186.48	389	174.38	378	12.11

Table S4: Glacier area, volume and change values per country. Data for P2 are from Hugonnet et al. (2021)**.**

Country	Area LIA (km^2)	Area 2015 (km^2)	Relative area change LIA-2015 (%)	Volume LIA (km^3)	Volume 2015 (km^3)	Relative volume change (%)	Mean elevation change (P3) (m)	Increase in volume change rate (%) (P2 vs. P1)
France	537.11	225.63	-58.0	33.64	12.21	-63.7	-42.55	65.4
Switzerland	1790.26	889.88	-50.3	133.51	59.33	-55.6	-40.93	59.5
Italy	967.82	318.59	-67.1	57.65	14.76	-74.4	-44.72	38.9
Austria	910.98	358.27	-60.7	56.00	13.32	-76.2	-47.03	38.3
Germany	3.36	0.30	-92.1	0.13	0.003	-97.8	-29.72	28.5
Slovenia	0.82		-100	0.02		-100	-21.90	

Table S5: Glacier area, volume and change values per basin. The basins of the Adige, Brenta, Piave, Tagliamento and Soča are listed together under south-eastern Alps. Data for P2 from Hugonnet et al. (2021)**.**

Basin	Area LIA (km^2)	Area 2015 (km^2)	Relative area change LIA-2015 (%)	Volume LIA (km^3)	Volume 2015 (km^3)	Volume change rate P1 (km^3 a^{-1})	Volume change rate P2 (km^3 a^{-1})	Increase in volume change rate (%) (P2 vs. P1)
Rhône	1480.97	781.47	-47.2	116.47	53.48	-0.36	-0.78	54.0
south-eastern Alps	345.32	92.01	-73.4	18.72	3.11	-0.10	-0.08	-16.5
Po	723.99	269.80	-62.7	44.20	13.06	-0.19	-0.23	17.2
Danube	1026.74	397.32	-61.3	61.51	15.13	-0.27	-0.30	9.8
Rhine	631.89	265.29	-58.0	40.04	14.85	-0.13	-0.29	54.6

2 Supplementary figures

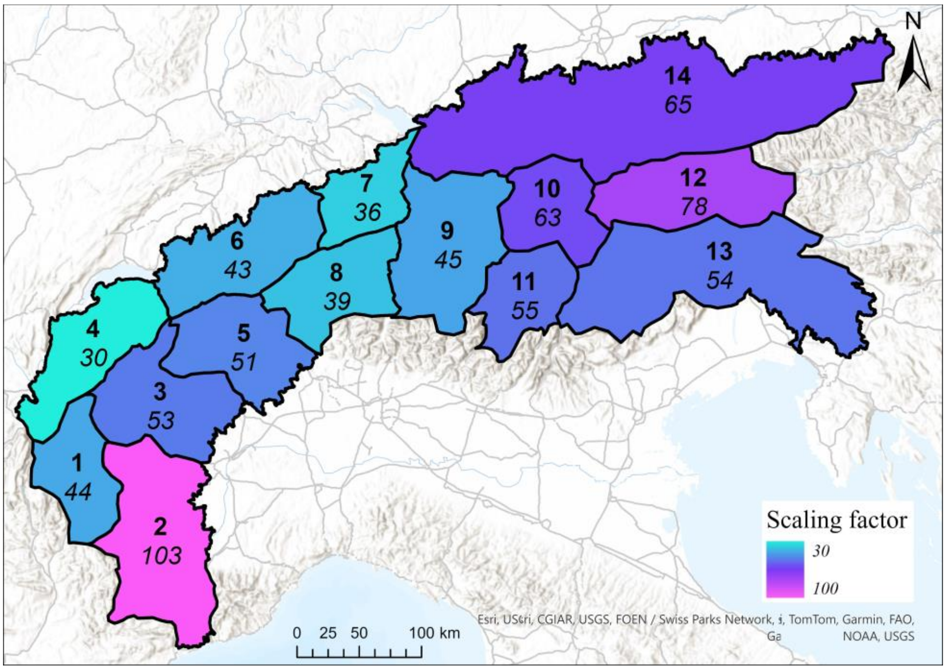

Figure S1: Region IDs (bold) and scaling factors (italic) used for the LIA surface reconstruction.

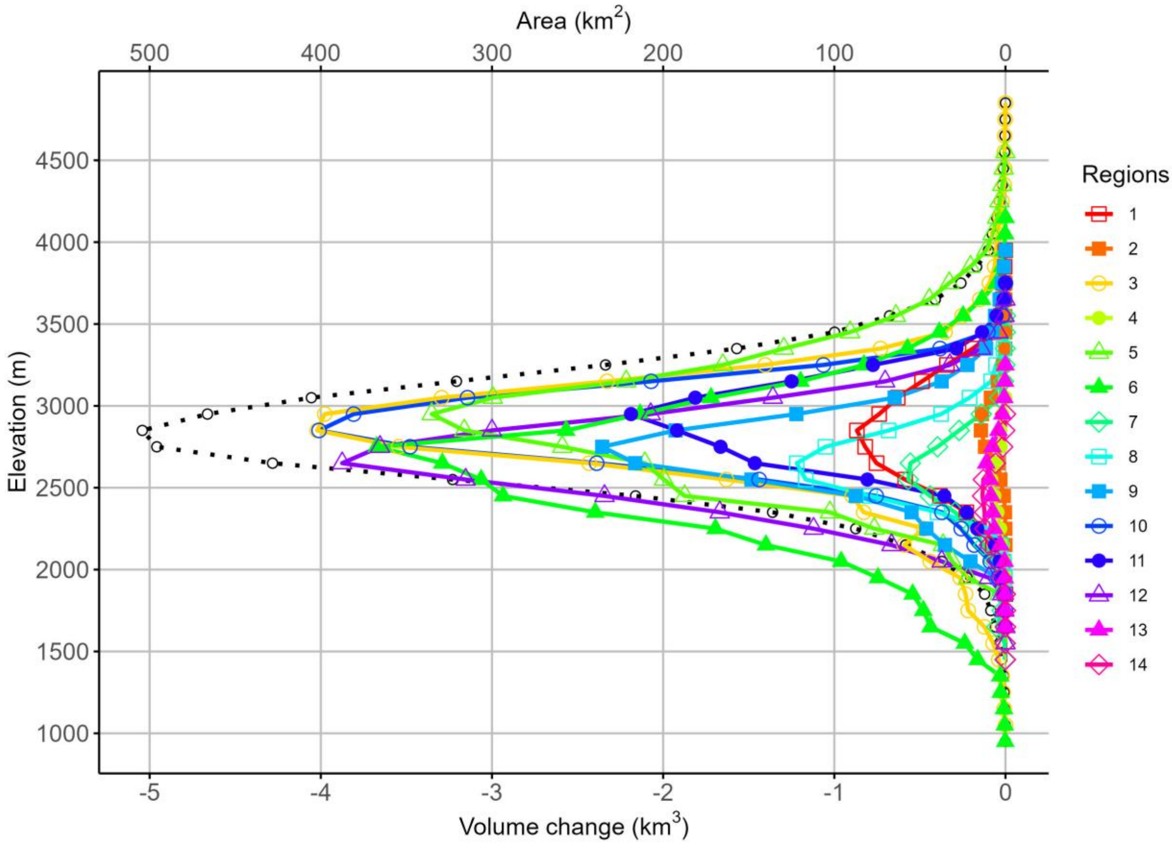

Figure S2: Volume change for the 14 subregions (the black dotted line indicates the area in the specific elevation).

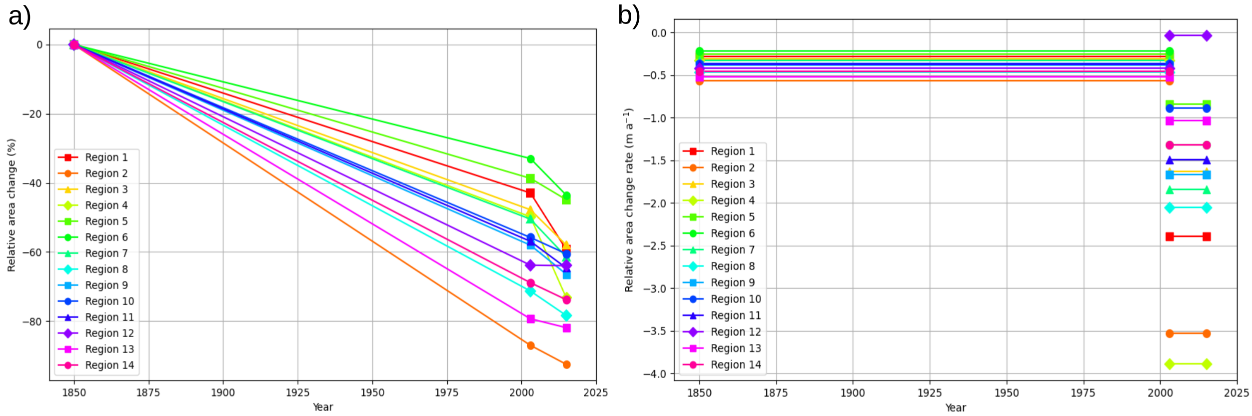

Figure S3: a) Relative glacier area change per region. b) relative area change rate per region.

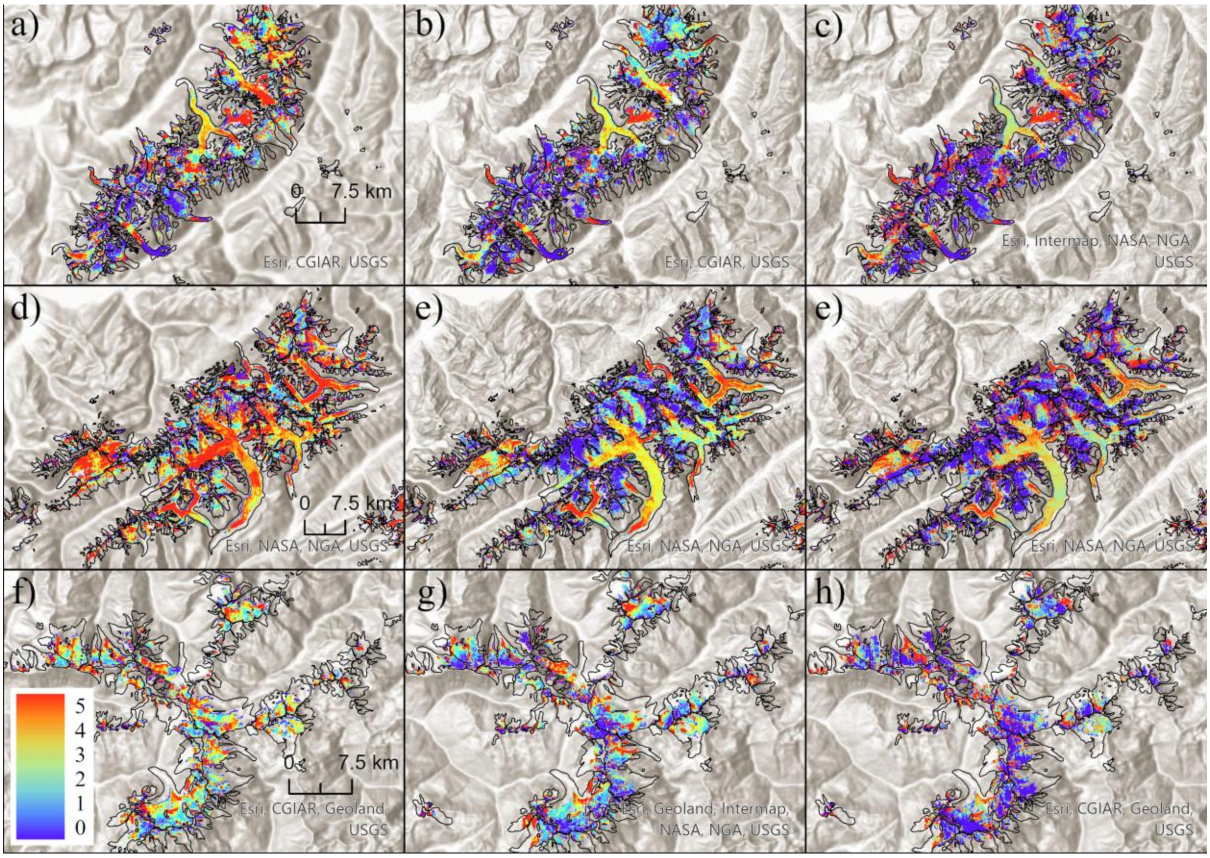

Figure S4: Acceleration rate after 2000 calculated for a), d), f) from Hugonnet et al. (2021), b), e), g) from Sommer et al. (2020) and c), e), h) from the difference of the SRTM DEM and the COP DEM. The mountain ranges are a-c) Mt. Blanc, d-e) Bernese Alps, f-h) Ortles range. All background images: ESRI, (2023a).

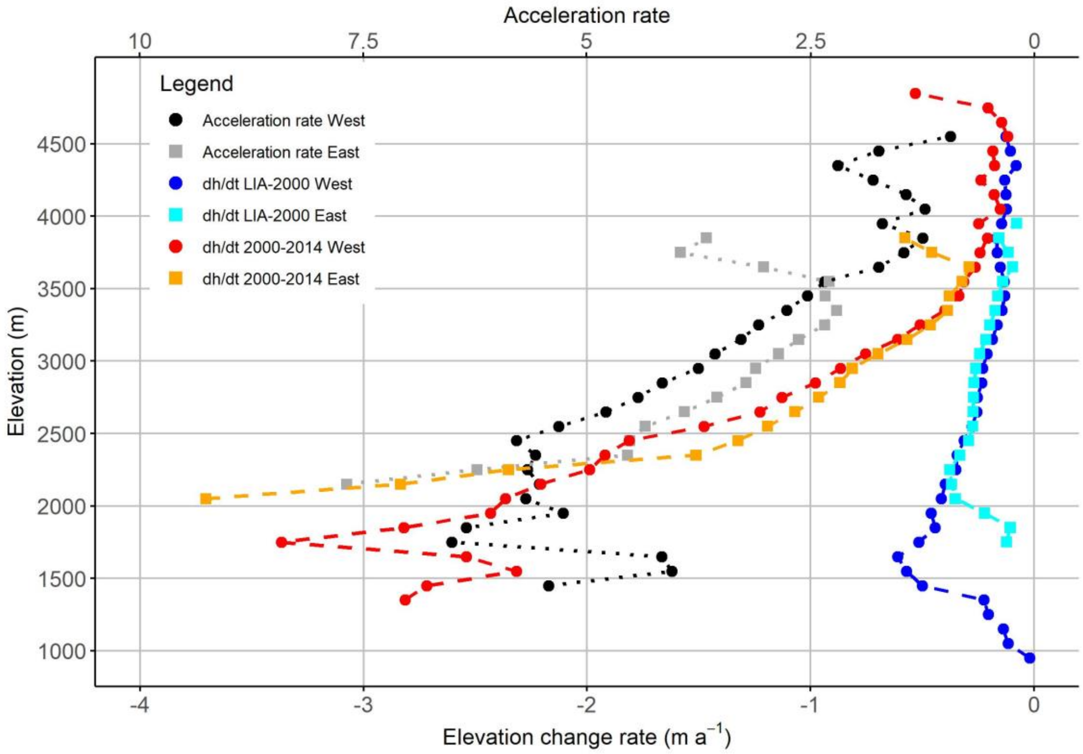

Figure S5: Elevation change rates LIA to 2000 (P1) and 2000 to 2014 (P2) from Hugonnet et al. (2021) as well as the acceleration rate for the eastern and western Alps.

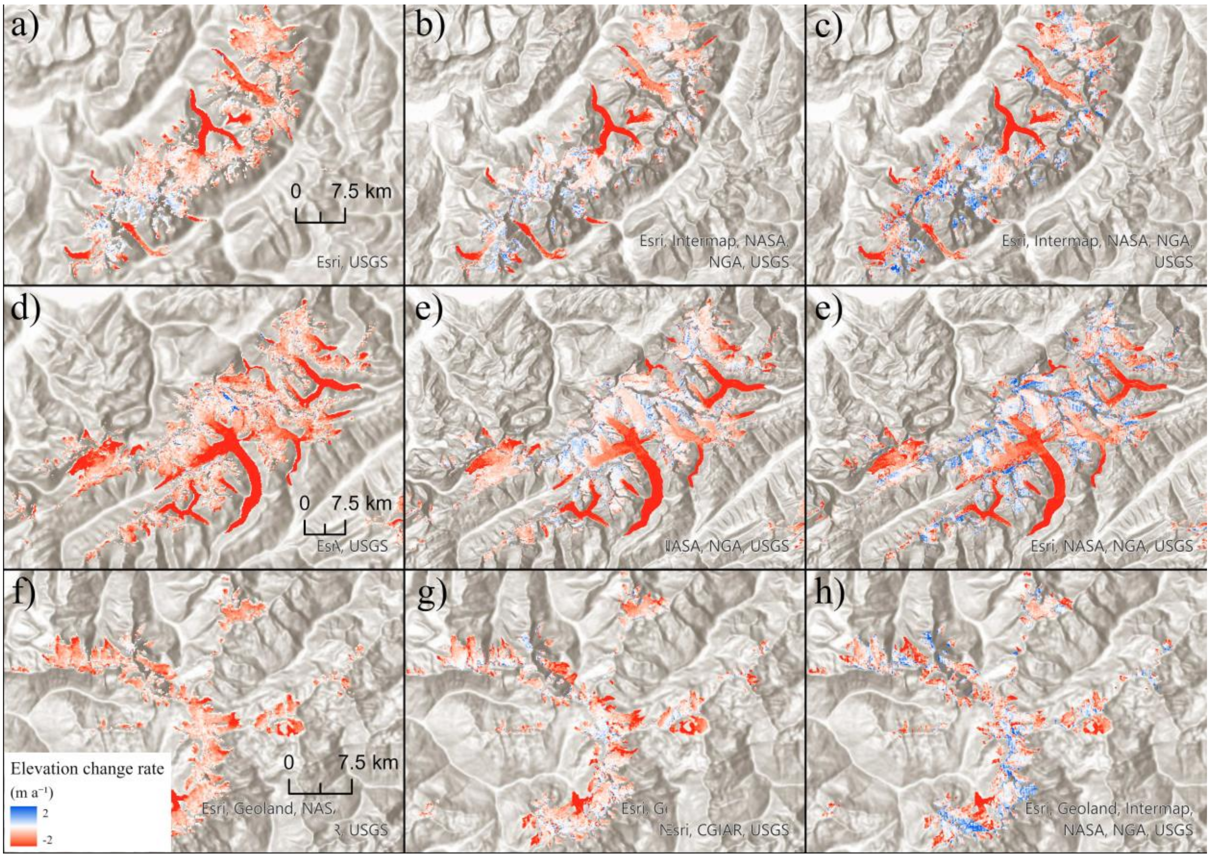

Figure S6: Elevation change rate (m) for P2 a), d), f) from Hugonnet et al. (2021), b), e), g) from Sommer et al. (2020) and c), e), h) from the difference of the SRTM DEM and the COP DEM. The mountain ranges are a-c) Mt. Blanc, d-e) Bernese Alps, f-h) Ortles range. All background images: ESRI, (2023a).

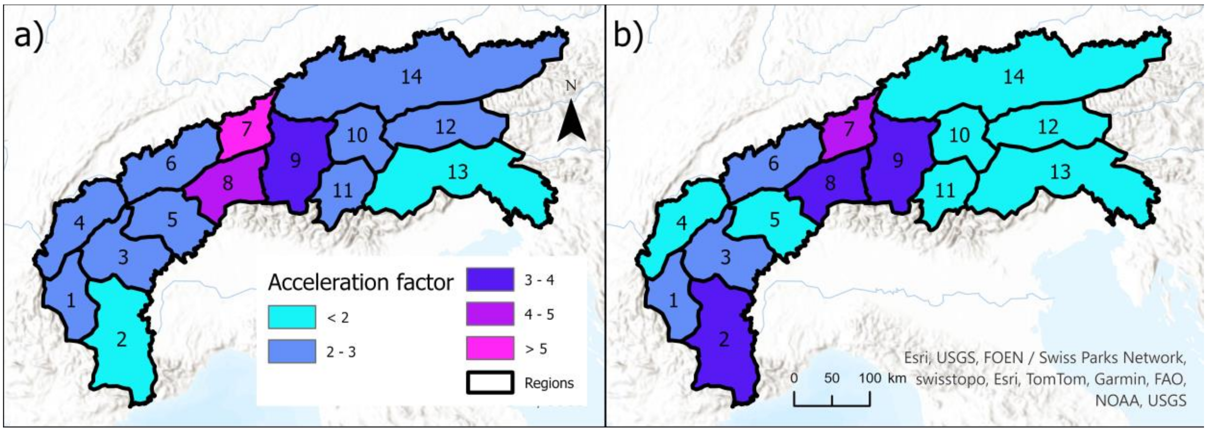

Figure S7: Acceleration factor from comparing elevation change rates of a) LIA to SRTM to Sommer et al. (2020) and b) LIA to SRTM compared to the SRTM to COP DEM period. All background images: ESRI, (2023a).

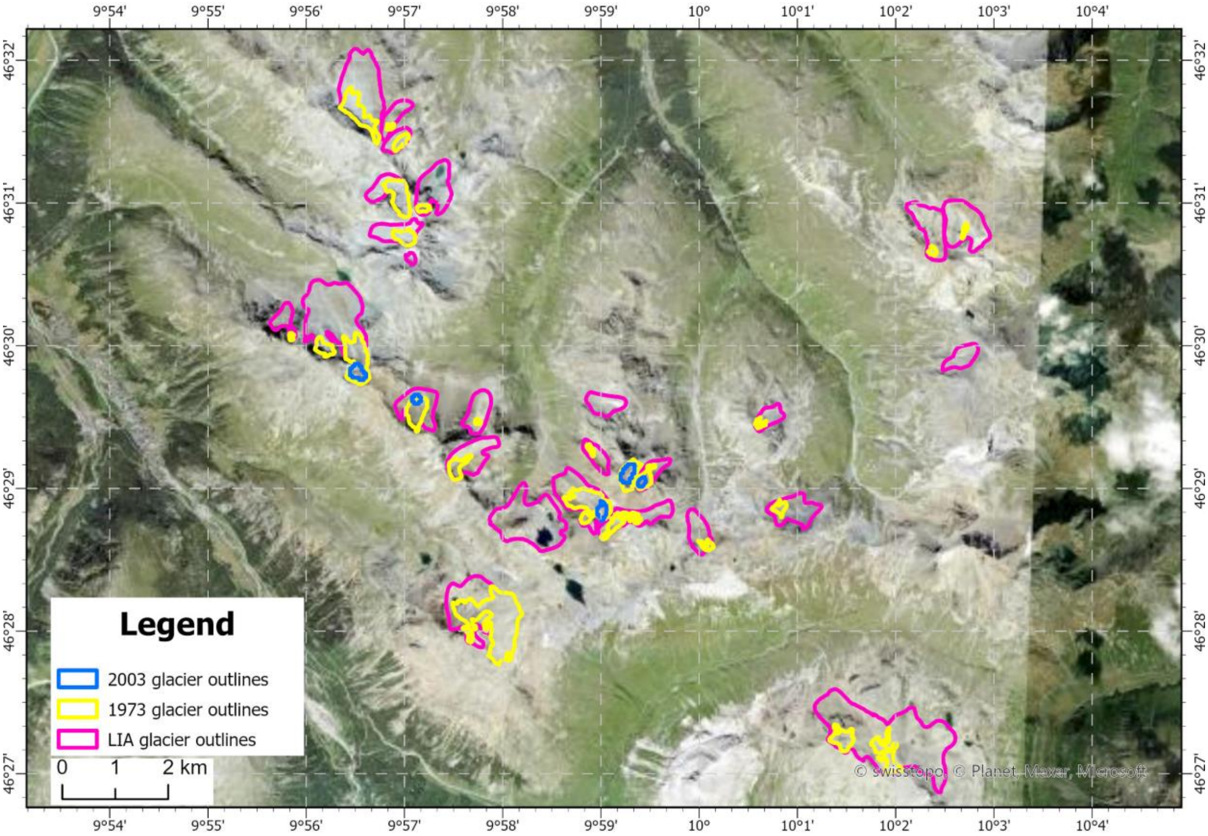

Figure S8: Examples of an already glacier-free (no glaciers in 2015) basin (Val Chamuera in Engadin, Switzerland). Background: ESRI, (2023b)**.**

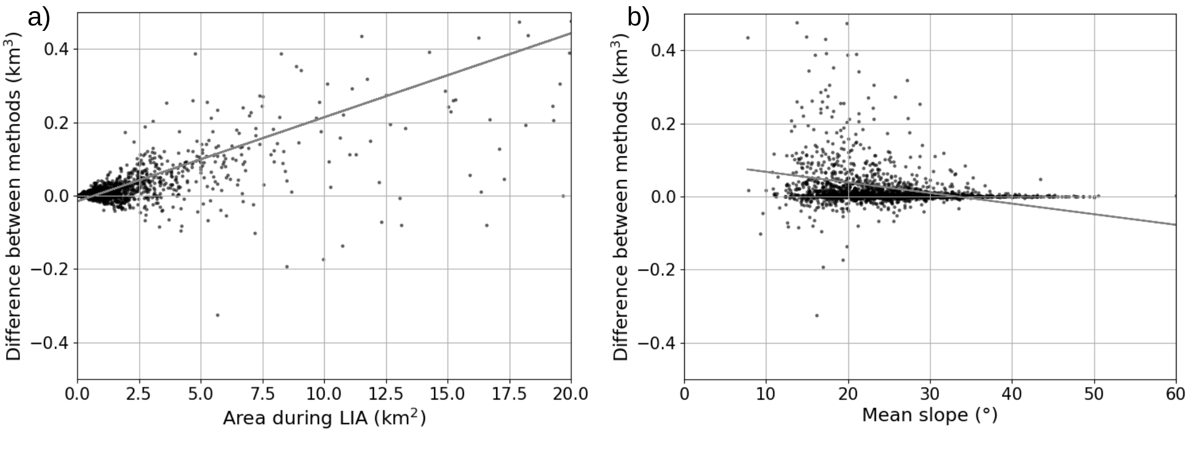

Figure S9: a) Difference in volume change (km^3) per glacier between the two methods (GIS-based and parameterisation scheme) against the initial area. b) The difference between the methods against the mean slope. Positive values indicate the calculated volume change in the GIS approach being larger.

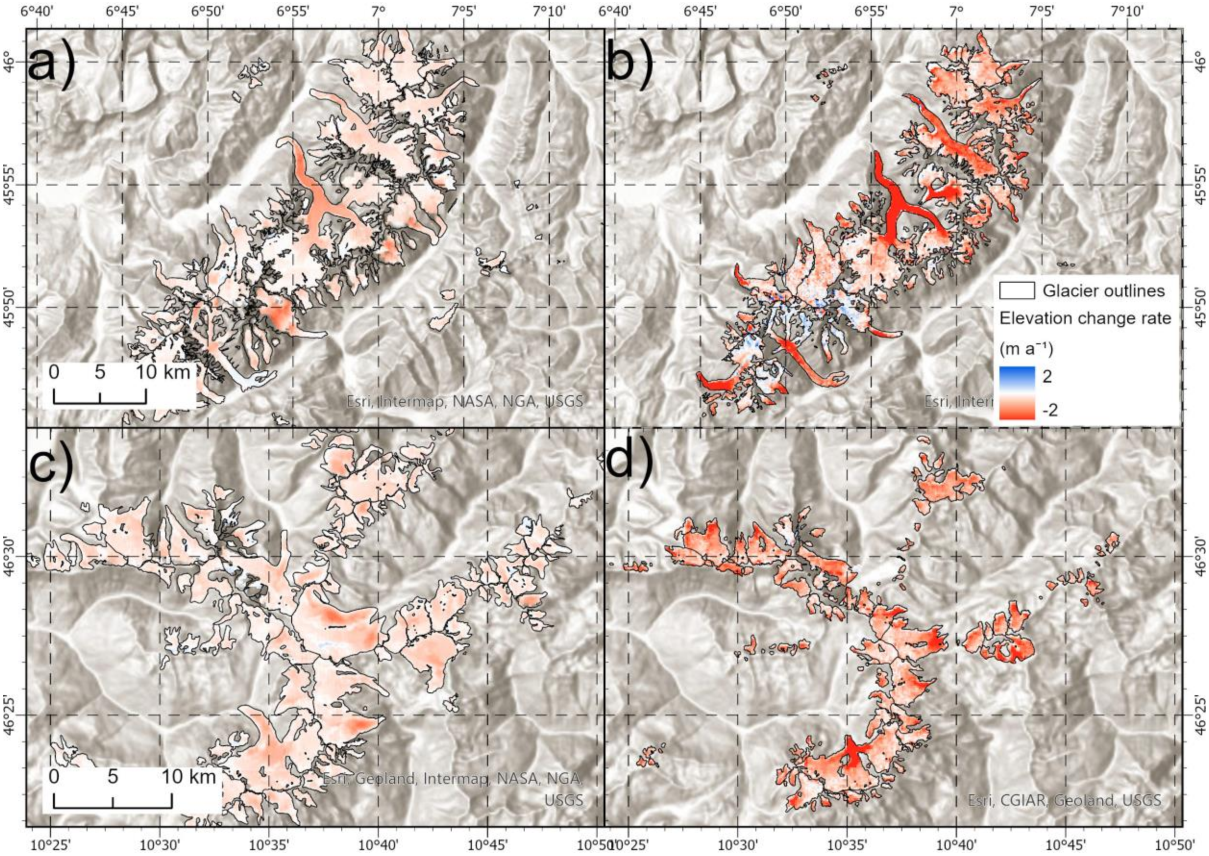

Figure S10: Examples of elevation change rates between the LIA and 2000 (P1) (a & c) and 2000-2014 (P2) after Hugonnet et al. (2021) (b & d) for the Mt. Blanc region (a & b) and the Ortles-Cevedale group (c & d) using the same colour legend for all panels. All background images: ESRI, (2023a)**.**

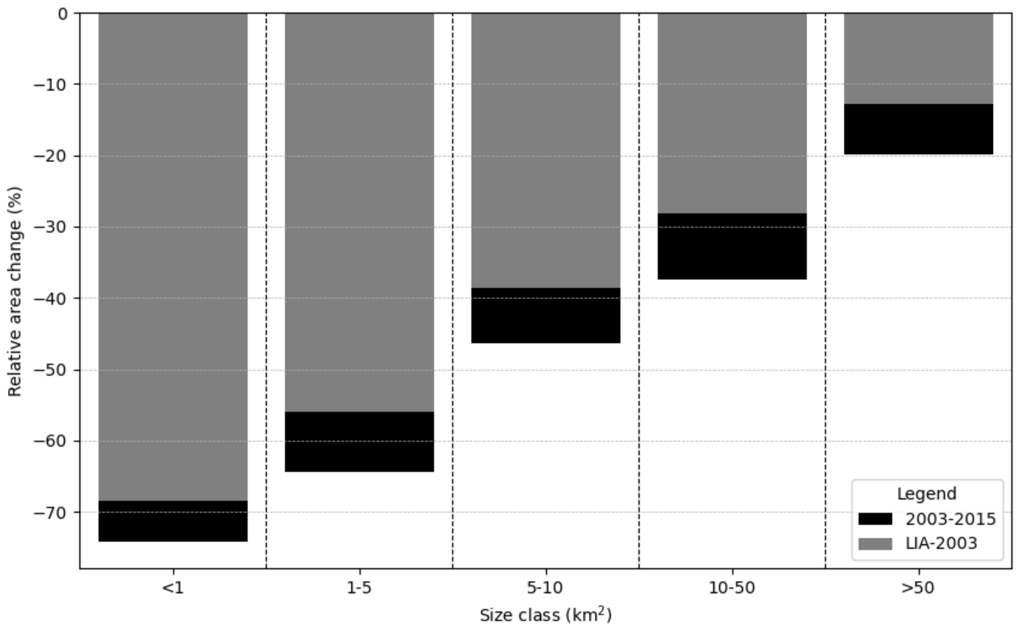

Figure S11: Relative glacier area changes per size class since the LIA.

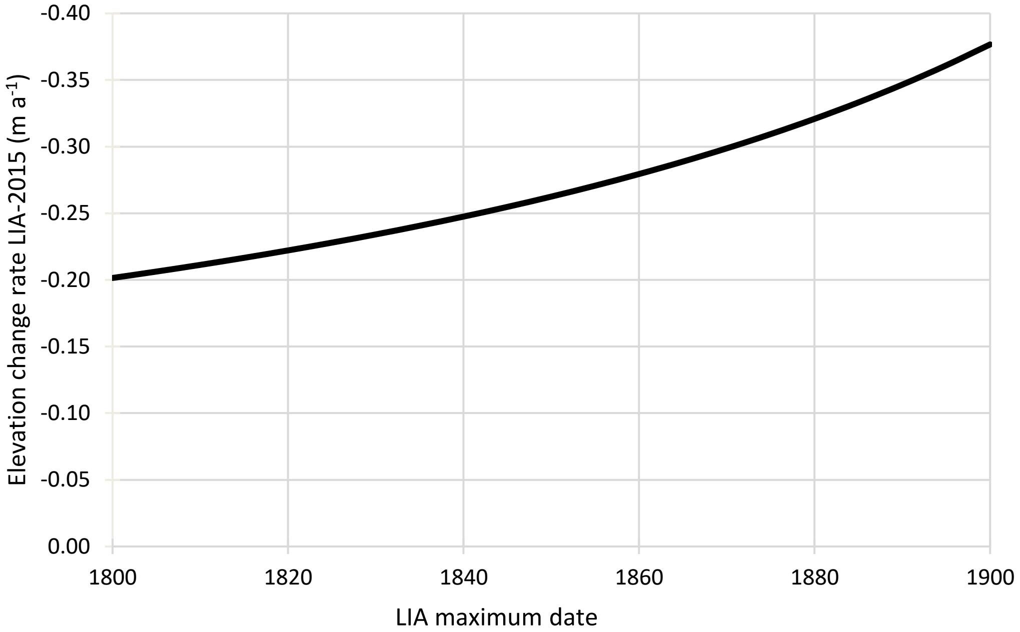

Figure S12: Effect of LIA starting date on elevation and volume change rates.

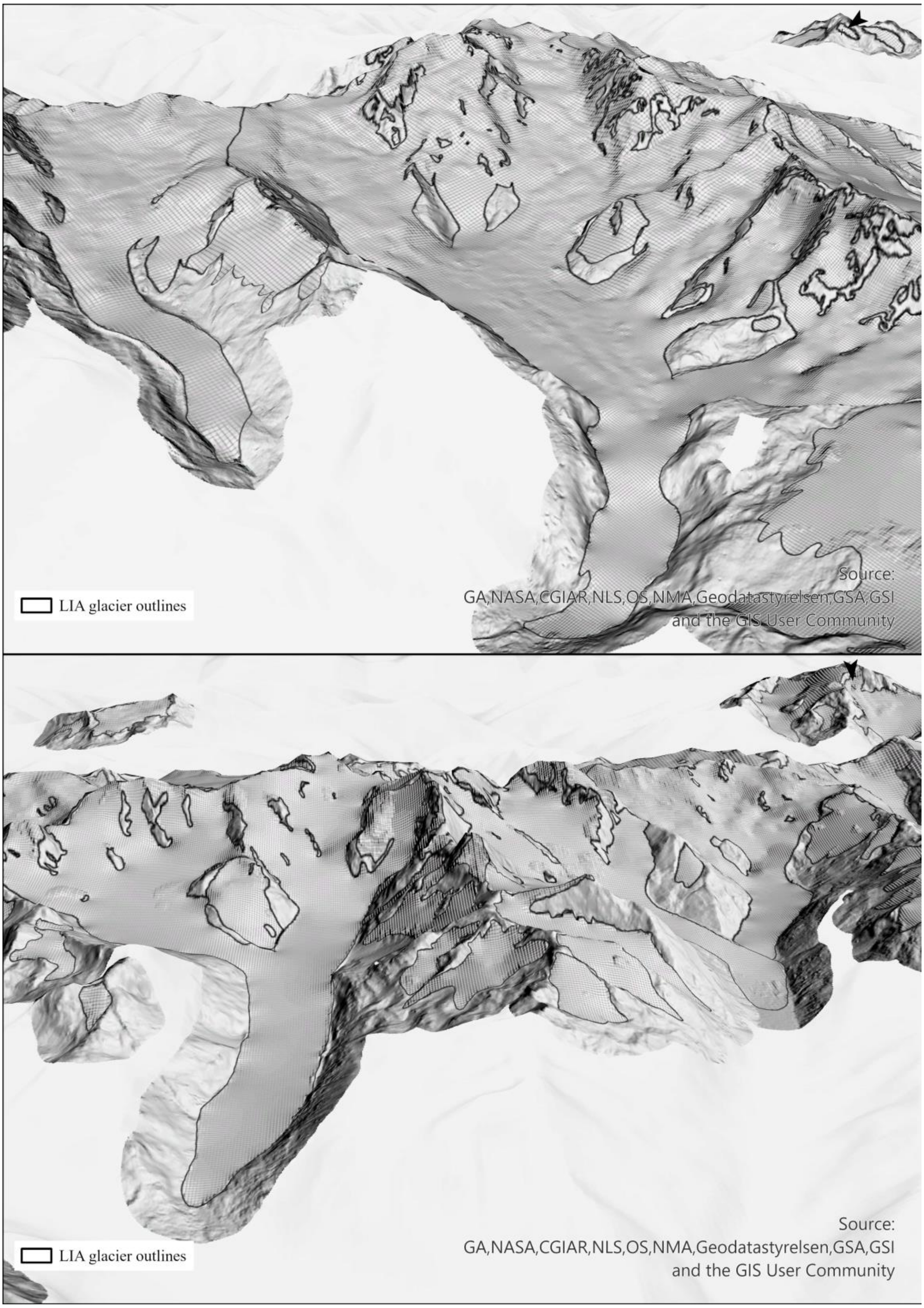

Figure S13: Hillshade of Monte Rosa and Bernina at the end of the LIA.

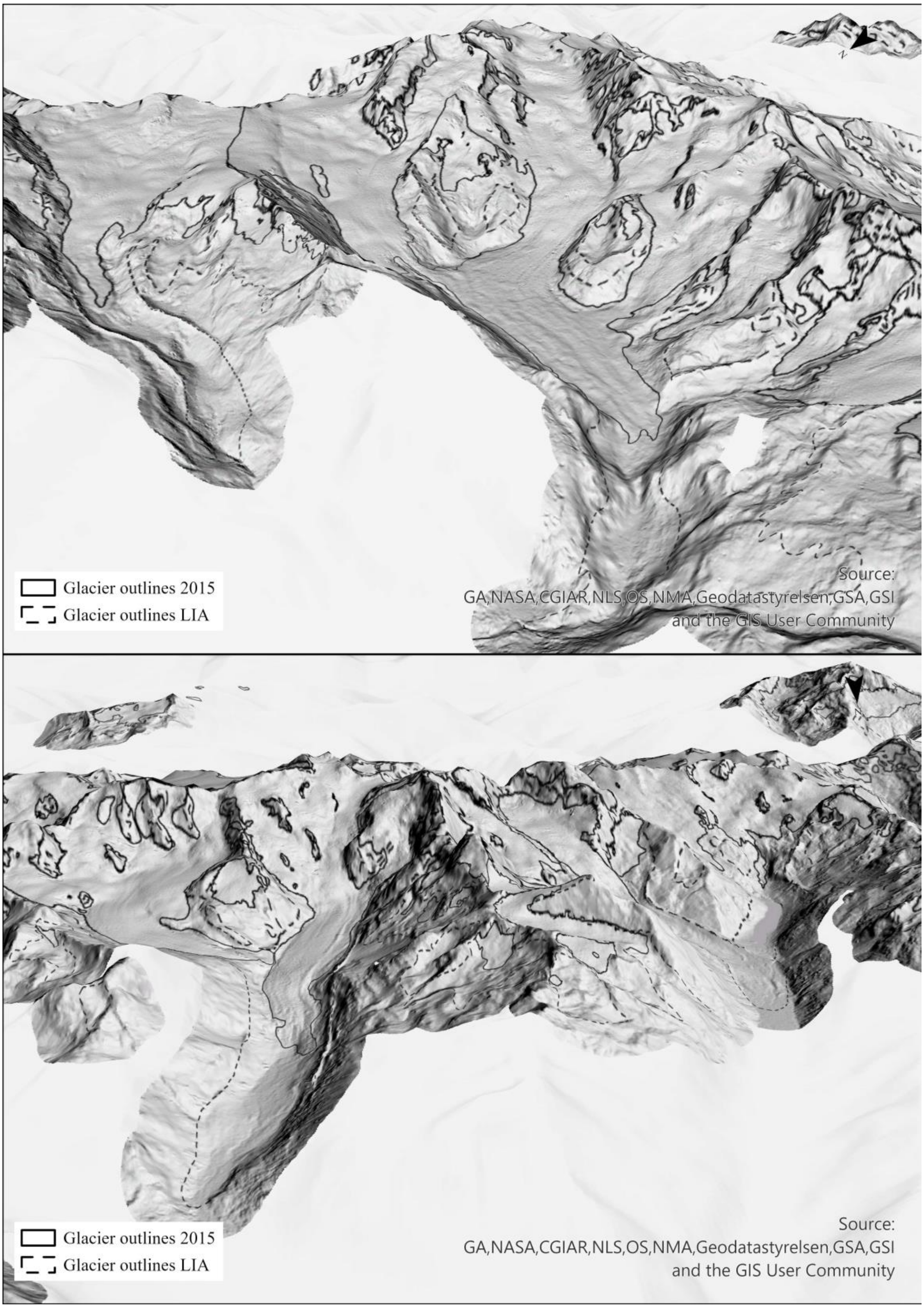

Figure S14: Hillshade of Monte Rosa and Bernina in 2015.

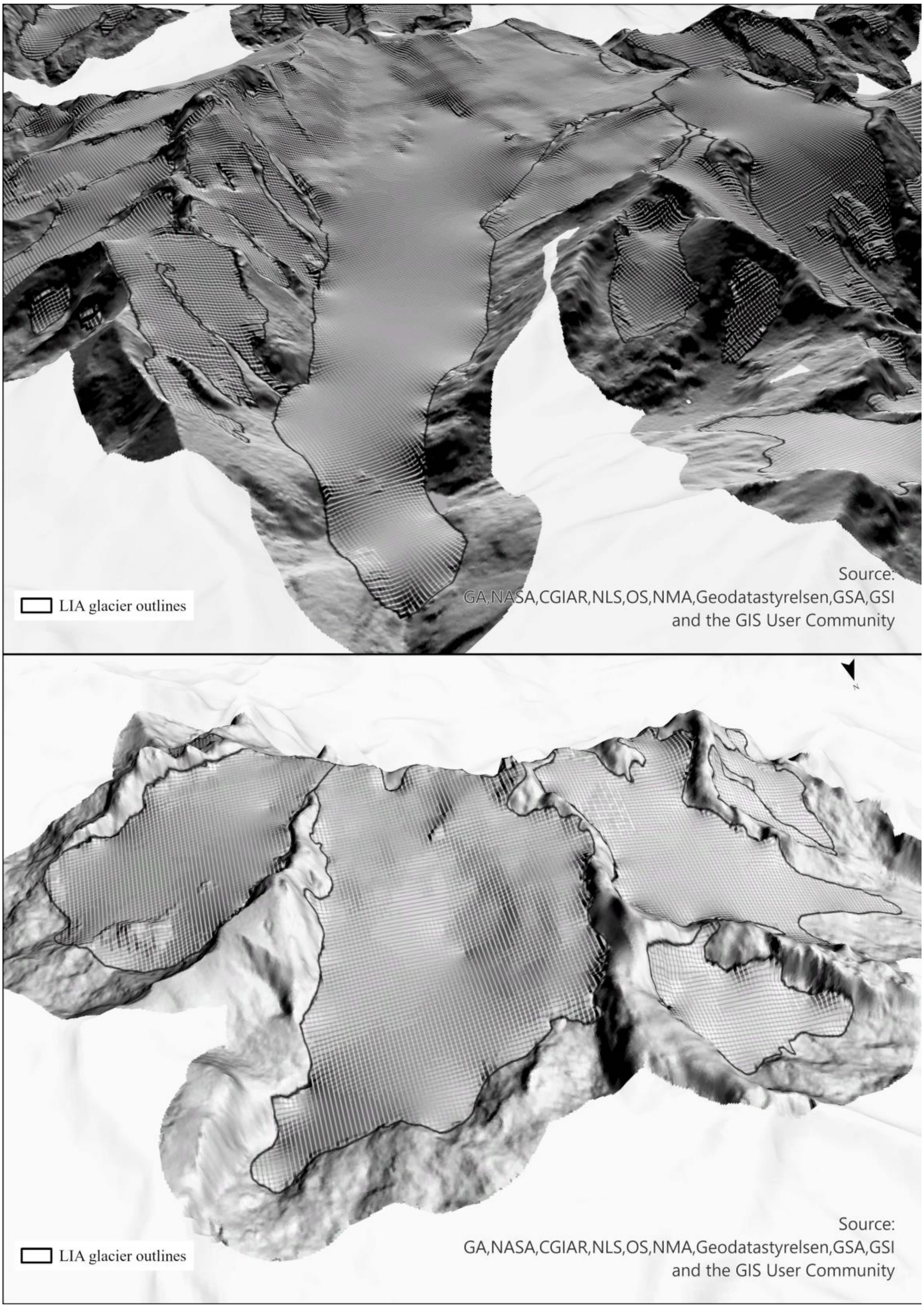

Figure S15: Hillshade of Pasterze and Dachstein at the end of the LIA.

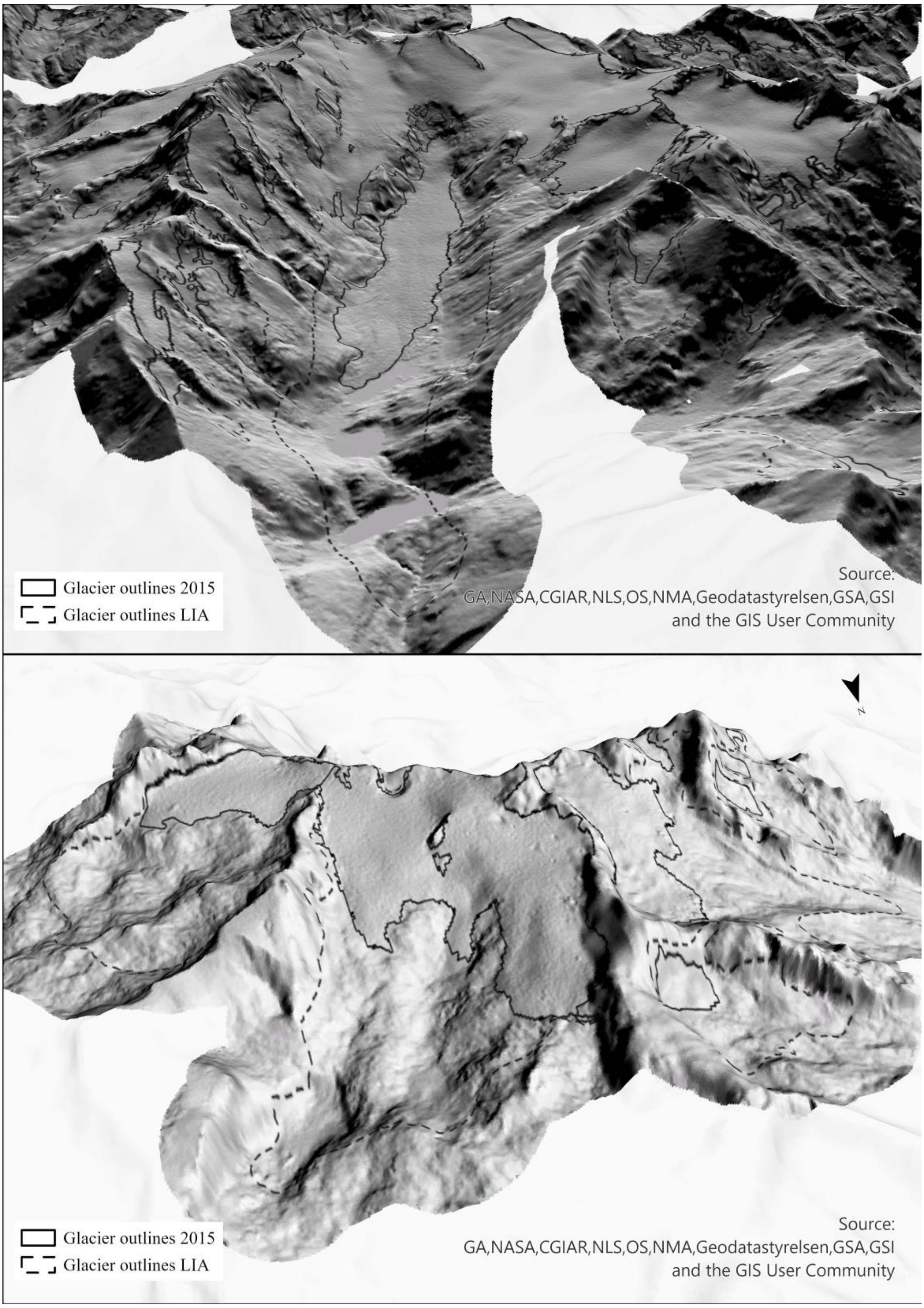

Figure S16: Hillshade of Pasterze and Dachstein in 2015.

3 Uncertainty calculation

The mapping uncertainty was taken from Reinthaler and Paul (2023) with a range of 10.1% or ±5.05% around the mean. This value was calculated from two multiple digitising experiments regarding interpretation and reproduction uncertainty. This would give a total volume of 281±14.2 km^3.

The values regarding the uncertainty of the surface reconstruction were taken from Reinthaler and Paul (subm.) as the mean difference (m) between the reconstructed LIA surface of the Bernese Alps and the reference DEM (Dufour Atlas). A change of the mean glacier thickness by 4.6 m would lead to a change in the total volume of 6.9% (281±19.4 km^3).

The uncertainty values relating to the ice thickness (bedrock) data were taken directly from the studies publishing the datasets and applied to the LIA dataset. For glaciers from the study by Helfricht et al. (2019), the uncertainty value of 5% on the total volume taken and for the study by Grab et al. (2021), 4.1%. For the remaining glaciers, the uncertainty was according to Millan et al. (2022) conservatively estimated to be 30% of the total volume. The resulting volume uncertainty for the entire area is 12.7% with a total volume of 281±35 km^3 (Table S6).

Table S6: Uncertainty calculation of the impact of the ice thickness dataset on the total volume.

Country	LIA volume (km^3)	Ice thickness dataset	Uncertainty value (%)	Lower bound LIA volume (km^3)	Upper bound LIA volume (km^3)
FR	33.64	(Millan et al., 2022)	30	23.55	43.73
CH	133.51	(Grab et al., 2021)	4.1	128.04	138.99
IT	57.65	(Millan et al., 2022)	30	40.35	74.94
AT	56.00	(Helfricht et al., 2019)	5	53.20	58.80
DE	0.13	(Millan et al., 2022)	30	0.09	0.17
SI	0.02		30	0.01	0.02
Total	281.0		12.7	245.3	361.6

The total random error (ε) composed of mapping, surface reconstruction and bedrock uncertainty, was calculated as $\varepsilon = \sqrt{(5.05^2 + 6.9^2 + 12.7^2)}$ and results in 15.3% and a total volume of 281±43 km^3.

On top of the upper bound of 324 km^3, an underestimation of 0.24 km^3 occurs from glaciers without LIA equivalent. The total area in the RGI v7.0 is 12.1 km^2 and with a relative change of 68.4% for glaciers smaller than 1 km^2 this leads to a total LIA area of 38.37 km^2. The LIA volume was calculated by using the 2015 mean glacier thickness (h_F, calculated from the parameterisation scheme) and the LIA area. Glaciers completely melted away are according to Parkes and Marzeion (2018) responsible for 4.4 mm (lower bound) of sea level rise compared to a total of 89.1 mm between 1901 and 2015. This is a 4.9% difference and would add an additional 13.9 km^3 and together with the 0.24 km^3 gives a potential underestimation of 14.1 km^3. Taking all factors into account, the upper limit for the total volume would be 338 km^3.

4 Parameter calculations:

1. Calculate length [$L0$] of each glacier Lo taken from centrelines using OGGM script. Length of the ablation area [La]= $L0$/2.
2. Calculate min and max elevation for each glacier.
3. Elevation range $dH = H_{max} - H_{min}$.
4. Calculate average slope a = aretan[$\frac{dH}{Lo}$] .
5. Mean basal shear stress: $\tau_f = 0.005 + 1.598 * dH - 0.435 * dH$.
6. Average ice depth along the flowline $h_f = \frac{\tau_f}{f \rho g \sin \alpha}$ where the shape factor f = 0.8; g is the gravitational acceleration 9.81 m s^{-2}; and p = the ice density (900 kg m^{-3}).
7. Average thickness for a semi-elliptical profile: $h_F = (\frac{\pi}{4}) h_f$.
8. Volume $V = A * h_F$; A being the glacier area.
9. Temperature changes from ELA changes: $\delta T = \frac{\delta ELA}{\text{lr}}$ lr being the lapse rate.

5 Additional references

Colucci, R. R. and Žebre, M.: Late Holocene evolution of glaciers in the southeastern Alps, J Maps, 12, 289–299, https://doi.org/10.1080/17445647.2016.1203216, 2016.

ESRI: “Topographic” [basemap]. scale not given. “World Topographic Map,” 2023a.

ESRI: “World Imagery” [basemap]. scale not given. “World Imagery,” 2023b.

Fischer, A., Seiser, B., Stocker Waldhuber, M., Mitterer, C., and Abermann, J.: Tracing glacier changes in Austria from the Little Ice Age to the present using a lidar-based high-resolution glacier inventory in Austria, Cryosphere, 9, 753–766, https://doi.org/10.5194/tc-9-753-2015, 2015.

Gardent, M. and Deline, P.: Stages of glacial retreat in the French Alps since the termination of the Little Ice Age, https://doi.org/10.1016/j.quaint.2012.08.184, 2011.

Grab, M., Mattea, E., Bauder, A., Huss, M., Rabenstein, L., Hodel, E., Linsbauer, A., Langhammer, L., Schmid, L., Church, G., Hellmann, S., Deleze, K., Schaer, P., Lathion, P., Farinotti, D., and Maurer, H.: Ice thickness distribution of all Swiss glaciers based on extended ground-penetrating radar data and glaciological modeling, Journal of Glaciology, 67, 1074–1092, https://doi.org/10.1017/jog.2021.55, 2021.

Groß, G.: Der Flächenverlust der Gletscher in Österreich 1850 – 1920 – 1969, Zeitschrift für Gletscherkunde und Glazialgeologie, 23, 131–141, 1987.

Helfricht, K., Huss, M., Fischer, A., and Otto, J. C.: Calibrated ice thickness estimate for all glaciers in Austria, Front Earth Sci (Lausanne), 7, 1–15, https://doi.org/10.3389/feart.2019.00068, 2019.

Hugonnet, R., McNabb, R., Berthier, E., Menounos, B., Nuth, C., Girod, L., Farinotti, D., Huss, M., Dussaillant, I., Brun, F., and Kääb, A.: Accelerated global glacier mass loss in the early twenty-first century, Nature, 592, 726–731, https://doi.org/10.1038/s41586-021-03436-z, 2021.

Knoll, C., Kerschner, H., Heller, A., and Rastner, P.: A GIS-based reconstruction of little ice age glacier maximum extents for South Tyrol, Italy, Transactions in GIS, 13, 449–463, https://doi.org/10.1111/j.1467-9671.2009.01173.x, 2009.

Lucchesi, S., Fioraso, G., Bertotto, S., and Chiarle, M.: Little Ice Age and contemporary glacier extent in the Western and South-Western Piedmont Alps (North-Western Italy), J Maps, 10, 409–423, https://doi.org/10.1080/17445647.2014.880226, 2014.

Maisch, M., Wipf, A., Denneler, B., Battaglia, J., and Benz, C.: Die Gletscher der Schweizer Alpen: Gletscherhochstand 1850, aktuelle Vergletscherung, Gletscherschwundszenarien, in: Schlussbericht NFP 31, second edition, Hochschulverlag ETH Zurich, Zurich, 373p, 2000.

Millan, R., Mouginot, J., Rabatel, A., and Morlighem, M.: Ice velocity and thickness of the world’s glaciers, Nat Geosci, 15, 124–129, https://doi.org/10.1038/s41561-021-00885-z, 2022.

Müller, F., Caflisch, T., and Müller, G.: Firn und Eis der Schweizer Alpen: Gletscherinventar, Geographisches Institut Publ. 57, Zurich, Eidgenössische Technische Hochschule, 1976.

Parkes, D. and Marzeion, B.: Twentieth-century contribution to sea-level rise from uncharted glaciers, Nature, 563, 551–554, https://doi.org/10.1038/s41586-018-0687-9, 2018.

Paul, F., Rastner, P., Azzoni, R. S., Diolaiuti, G., Fugazza, D., Bris, R. Le, Nemec, J., Rabatel, A., Ramusovic, M., Schwaizer, G., and Smiraglia, C.: Glacier shrinkage in the Alps continues unabated as revealed by a new glacier inventory from Sentinel-2, Earth Syst Sci Data, 12, 1805–1821, https://doi.org/10.5194/essd-12-1805-2020, 2020.

Pfeffer, W. T., Arendt, A. A., Bliss, A., Bolch, T., Cogley, J. G., Gardner, A. S., Hagen, J. O., Hock, R., Kaser, G., Kienholz, C., Miles, E. S., Moholdt, G., Mölg, N., Paul, F., Radić, V., Rastner, P., Raup, B. H., Rich, J., Sharp, M. J., Andreassen, L. M., Bajracharya, S., Barrand, N. E., Beedle, M. J., Berthier, E., Bhambri, R., Brown, I., Burgess, D. O., Burgess, E. W., Cawkwell, F., Chinn, T., Copland, L., Cullen, N. J., Davies, B., De Angelis, H., Fountain, A. G., Frey, H., Giffen, B. A., Glasser, N. F., Gurney, S. D., Hagg, W., Hall, D. K., Haritashya, U. K., Hartmann, G., Herreid, S., Howat, I., Jiskoot, H., Khromova, T. E., Klein, A., Kohler, J., König, M., Kriegel, D., Kutuzov, S., Lavrentiev, I., Le Bris, R., Li, X., Manley, W. F., Mayer, C., Menounos, B., Mercer, A., Mool, P., Negrete, A., Nosenko, G., Nuth, C., Osmonov, A., Pettersson, R., Racoviteanu, A., Ranzi, R., Sarikaya, M. A., Schneider, C., Sigurdsson, O., Sirguey, P., Stokes, C. R., Wheate, R., Wolken, G. J., Wu, L. Z., and Wyatt, F. R.: The randolph glacier inventory: A globally complete inventory of glaciers, Journal of Glaciology, 60, 537–552, https://doi.org/10.3189/2014JoG13J176, 2014.

Reinthaler, J. and Paul, F.: Using a Web Map Service to map Little Ice Age glacier extents at regional scales, Ann Glaciol, 1–19, https://doi.org/https://doi.org/10.1017/ aog.2023.39, 2023.

Reinthaler, J. and Paul, F.: Methods for reconstructing Little Ice Age glacier surfaces in Novaya Zemlya and the Swiss Alps: Uncertainties and volume changes, Geomorphology, https://doi.org/10.2139/ssrn.4593636, n.d.

RGI 7.0 Consortium: Randolph Glacier Inventory - A Dataset of Global Glacier Outlines, Version 7.0, https://doi.org/10.5067/f6jmovy5navz, 2023.

Sommer, C., Malz, P., Seehaus, T. C., Lippl, S., Zemp, M., and Braun, M. H.: Rapid glacier retreat and downwasting throughout the European Alps in the early 21st century, Nat Commun, 11, https://doi.org/10.1038/s41467-020-16818-0, 2020.

Vivian, R.: Les glacier des Alpes occidentales, Grenoble: Allier, 1975.

Zanoner, T., Carton, A., Seppi, R., Carturan, L., Baroni, C., Salvatore, M. C., and Zumiani, M.: Little Ice Age mapping as a tool for identifying hazard in the paraglacial environment: The case study of Trentino (Eastern Italian Alps), Geomorphology, 295, 551–562, https://doi.org/10.1016/j.geomorph.2017.08.014, 2017.